www.ptcer.pl/mccm

MATERIAŁY CERAMICZNE /CERAMIC MATERIALS/, 69, 3, (2017), 264-271

Alumina-zirconia composites produced by filter pressing of zirconia and transition alumina nanopowders

Łukasz Zych[1]*, Mirella Azar[2], Jerome Chevalier[2], Vincent Garnier[2], Beata Macherzyńska[1], Waldemar Pyda[1]

[1]AGH University of Science and Technology, Faculty of Materials Science and Ceramics, Cracow, Poland
[2]Université de Lyon, INSA-Lyon, MATEIS CNRS UMR 5510, Villeurbanne, France
*e-mail: lzych@agh.edu.pl

Abstract

The aim of this work was production of dense, fine-grained zirconia toughened alumina composites by the filter pressing method. It is presumed that such composites may exhibit enhanced mechanical properties, comparing to the coarse-grained ones. Colloidal shaping methods, e.g. filter pressing, enable to produce materials with homogenous microstructures and uniform distribution of composite constituents, which facilitates their sintering process and may lead to dense materials with fine grains. Alumina–zirconia composites with various zirconia fractions (from 5 vol.% to 30 vol.%) were fabricated using a commercial transition alumina powder (Nanotek®) and a zirconia powder produced by the hydrothermal method. Both powders were mixed at given rates in water suspension, and then shaped using the filter pressing method. Homogeneity of green samples was investigated using mercury porosimetry. The sintering was carried out in conditions determined during dilatometric measurements, e.g. taking into account transformation of the alumina. Sintering behaviour of the samples was investigated by density measurements, XRD analysis and SEM observations. Hardness and fracture toughness (K_{IC}) of the sintered samples were determined using the Vickers indentation method.
Keywords: Nanopowders, Transition alumina, ZTA composites, Suspension, Filter pressing

KOMPOZYTY Al_2O_3-ZrO_2 WYTWARZANE ZA POMOCĄ PRASOWANIA FILTRACYJNEGO NANOPROSZKÓW DWUTLENKU CYRKONU I PRZEJŚCIOWYCH FORM TLENKU GLINU

Celem pracy było wytworzenie gęstych, drobnoziarnistych kompozytów Al_2O_3–ZrO_2 (ZTA) przy wykorzystaniu metody prasowania filtracyjnego. Zakłada się, że takie kompozyty mogą wykazywać lepsze właściwości mechaniczne w porównaniu z kompozytami o mikrostrukturze składającej się z ziaren o większym rozmiarze. Metody formowania oparte na zawiesinach, np. prasowanie filtracyjne, pozwalają na wytwarzanie materiałów o jednorodnej mikrostrukturze i równomiernym rozmieszczeniu składników kompozytu. Taka mikrostruktura wyjściowych materiałów ułatwia proces ich spiekania, którego efektem mogą być gęste materiały o drobnych ziarnach. Kompozyty Al_2O_3–ZrO_2 o różnym udziale tlenku cyrkonu (od 5% do 30% obj.) zostały wytworzone z komercyjnego proszku przejściowej odmiany tlenku glinu (Nanotek®) oraz proszku tlenku cyrkonu otrzymanego metodą hydrotermalną. Proszki zostały wymieszane w ustalonych proporcjach w wodnej zawiesinie, a następnie uformowane metodą prasowania filtracyjnego. Jednorodność mikrostruktury surowych materiałów była określana metodą porozymetrii rtęciowej. Spiekanie kompozytów odbywało się w temperaturze określonej na podstawie pomiarów dylatometrycznych, tzn. biorąc pod uwagę przemianę fazową tlenku glinu. Zachowanie się materiałów podczas spiekania było badane poprzez określenie gęstości, analizę fazową XRD oraz obserwacje SEM. Twardość oraz odporność kompozytów na kruche pękanie (K_{IC}) wyznaczano metodą Vickersa.
Słowa kluczowe: nanoproszki, przejściowy tlenek glinu, kompozyty ZTA, zawiesina, prasowanie filtracyjne

1. Introduction

Ceramic matrix composites from the alumina-zirconia system are most widely investigated ones due to their mechanical properties especially high toughness, which is mainly achieved by transformation of zirconia from the tetragonal to monoclinic polymorph in the vicinity of a propagating crack tip [1]. More recently the research interest has focused on production of ceramics with grains getting a nanometric range since nano-materials are expected to exhibit different and better properties than conventional ones [2, 3]. That is why routes of preparation of the composites with submicrometric or even nanometric microstructures are sought. In general, production of dense, fine-grained ceramic materials requires fine starting powders, and a shaping technique which provides uniform microstructure of green bodies which in turn facilitates their further sintering, and enables to restrain the grain growth [2]. It is well known that colloidal processing of ceramic powders leads to very uniform microstructures of green bodies [4]. This approach was also successfully applied for the shaping of nanopowders [5–8]. Processing of powders in the suspension state provides better control of the state of homogenisation in composite systems, e.g. by adjusting the suspension pH [4].

Nanometric alumina powders often consist of transition phases such as γ or δ which undergo the phase transformation to thermodynamically stable α phase during sintering. This transformation occurs via a nucleation and growth process, and is generally accompanied by vermicular microstructures, showing a high proportion of intragranular pores [9]. The natural sintering of such powders leads to materials with micrometric grains. It was shown that colloidal processing of

ISSN 1505-1269

the transition alumina powders leads to better sintering results than dry pressing, when used as the shaping method [6]. However, in the literature, there is a lack of data concerning application of the transition alumina powders for production of composites from the Al_2O_3–ZrO_2 system, especially the ones containing higher amounts of zirconia [10].

This work aims for the attempt to produce alumina–zirconia composites using transition alumina and zirconia nanopowders that were shaped by a filter pressing technique, and to investigate an influence of the presence of zirconia nanoparticles on phase transformation and sintering of the transition alumina powder.

2. Experimental

As initial materials, a nanometric commercial transition alumina powder (NanoTek® Nanophase Technologies corp., Romeoville IL, USA) and nanometric undoped zirconia one were used. The latter one was produced by hydrothermal crystallization performed for 4 h at 250°C, as in detail described in Ref. [7]. The zirconia nanopowder after the synthesis was kept in a distilled water suspension in order to prevent formation of strong agglomerates during drying. The powders were characterised by the TEM (JEOL 200 CX, Tokyo, Japan), BET (Nova 1200e, Quantachrome Inc.), DLS (Zetasizer Nano-ZS, Malvern Inc.) and XRD (RIGAKU vertical diffractometer, Kent, UK) techniques. The relation between zeta potential and pH of the studied suspensions was determined using the LDV method (Zetasizer Nano-ZS, Malvern Inc.).

The powders were mixed in distilled water (solid mass content c.a. 15 vol.%) in proportions necessary to produce composites containing 5%, 10%, 20%, and 30% by volume of zirconia. The suspensions were electrostatically dispersed by adjusting their pH values to 3 with HNO_3, as indicated by the zeta potential measurements. The suspensions were subjected to a high energy ultrasonic agitation for 5 minutes, and then filter pressed under 3 MPa using an apparatus shown in Fig. 1. A diameter of the filter pressed samples was 30 mm, and their height varied from 3 mm to 5 mm; the samples were free from cracks. Before further experiments, each sample was first dried in a desiccator at room temperature, and then at 100°C in a drier, until constant weight was obtained.

Pore size distributions of the dried compacts were determined by using the mercury porosimetry technique (Autopore III, Micromeritics Inst.). In order to determine suitable sintering conditions, the samples were sintered in a dilatometer (SETARAM 1700, Caluire, France) up to 1700°C in air flow at a heating rate of 5°C/min.

The composite samples were isothermally sintered for 15 min at temperatures close to the alumina phase transformation, i.e. 1100°C, 1200°C and 1300°C. In order to find the best sintering conditions that result in the highest density of composite, the samples were sintered for 1 hour at 1600°C and 1700°C. In the case of pure alumina samples such final sintering temperatures led to extensive grain growth with the same level of densification, so the alumina samples were ultimately sintered for 2 hrs at 1500°C in order to produce dense materials with the finest possible grain size.

Apparent density of the sintered samples was measured using the buoyancy method, taking into account their phase composition and true densities of δ-Al_2O_3 and γ-Al_2O_3 (3.490 g/cm^3), α-Al_2O_3 (3.987 g/cm^3), monoclinic ZrO_2 (5.560 g/cm^3) and tetragonal ZrO_2 (6.100 g/cm^3). The phase composition of heat treated samples was determined by the XRD technique (Brüker D8 ADVANCE diffractometer, $CuK_{\alpha 1}$, 0.05 °/step). In the case of samples with open porosity, pore size distributions were measured by mercury porosimetry. A microstructure of fracture surfaces was observed using SEM (Jeol JSM-840A, FEI XL 30 ESEM). Hardness and fracture toughness (K_{IC}) of dense composites were measured by Vickers indentation (FV-700, Future Tech) under a load of 4.9 N and 49.05 N or 98.1 N, respectively. The respective load values were 4.9 N and 9.81 N for pure alumina sinters. Young's modulus of the materials was determined by the ultrasonic method (UZ-1, Inco-Veritas, Poland).

3. Results and discussion

The morphology of the zirconia and alumina nanopowders is shown in Fig. 2, and their characteristics are collected in Table 1. When measured from TEM microphotographs, a crystallite size of both nanopowders was below 100 nm, i.e., approximately 11 nm and 30 nm for zirconia and alumina, respectively. However, from the practical point of view, the particle size distribution determined by the DLS method was more interesting and useful, because it indicated the presence of large powder agglomerates in actual suspensions as shown in Fig. 3. The zirconia powder contained a small amount of agglomerates bigger than c.a. 4 μm; further studies did not indicate any detrimental effects caused by them. The transition alumina powder consisted of 70 wt.% of δ phase and 30 wt.% of γ one, and zirconia powder consisted of 8 wt.% of monoclinic phase and 92 wt.% of tetragonal one.

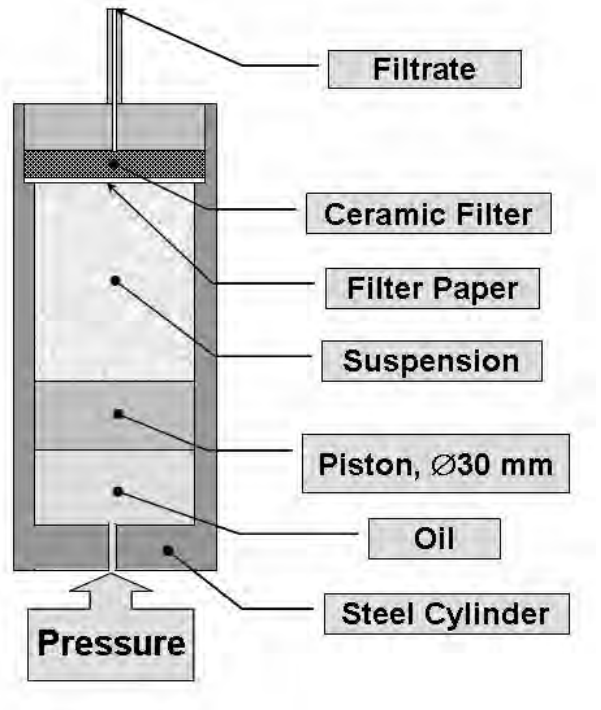

Fig. 1. A scheme of filter pressing apparatus.

The zeta potential vs. pH relationships shown in Fig. 4 enabled to find conditions of simultaneous dispersion of both powders. All mixtures of the powders were dispersed at pH 3, at which both powders showed relatively high positive zeta potential, which means that hetero-coagulation did not take place.

The suspensions of pure alumina and alumina with 5–30 vol.% of ZrO_2 nanopowder showed no sedimentation during handling, when dispersed at pH 3 with high energy ultrasounds. The filter pressed suspensions resulted in green samples with narrow pore size distributions (Fig. 5), which indicated their uniform microstructure. The presence of zirconia particles shifted the pore size distribution towards smaller pore sizes, as a result of filling large pores among alumina particles with nanozirconia.

The sintering behaviour of the filter pressed samples during non-isothermal heating up to 1700°C at 5°C/min is shown in Fig. 6. All samples showed the sintering behaviour being characteristic for transition alumina [9], and related to its transformation to the stable α-alumina form which resulted in a change of the sintering rate at the transformation temperature. A characteristic transformation temperature

Table 1. Characteristics of nanopowders.

Nanopowder	Specific surface area [m^2/g]	d_{BET}* [nm]	d_{TEM}* [nm]	Phase composition [wt.%]
Al_2O_3	35.3	49.1	30±26	δ : γ 30: 70
ZrO_2	100.8	9.9	11±3	tetragonal : monoclinic 92 : 8

**d_{BET} - equivalent particle size calculated from the value of specific surface area; d_{TEM} - average value for 50 measurements; ± - standard deviation*

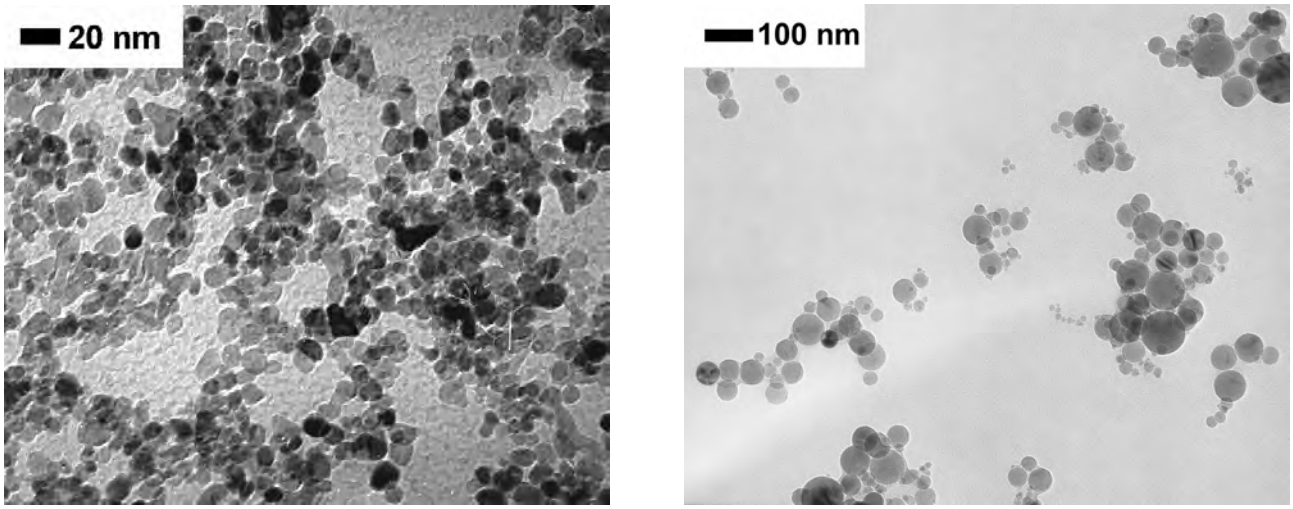

a) *b)*

Fig. 2. TEM microphotographs of zirconia nanopowder (a) and Nanotek alumina powder (b).

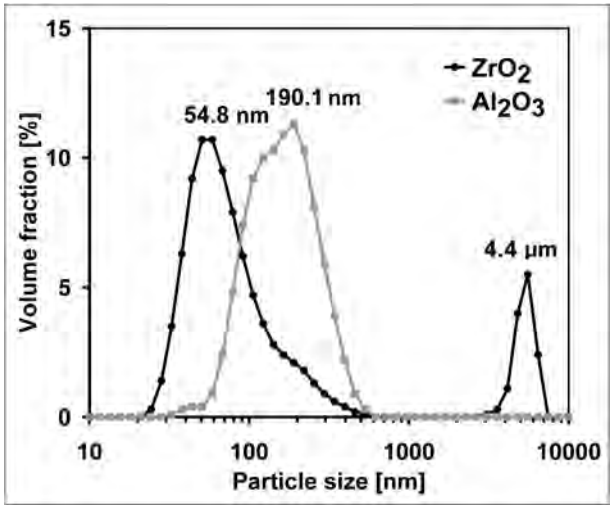

Fig. 3. Particle size distribution of alumina and zirconia nanopowders determined by DLS method.

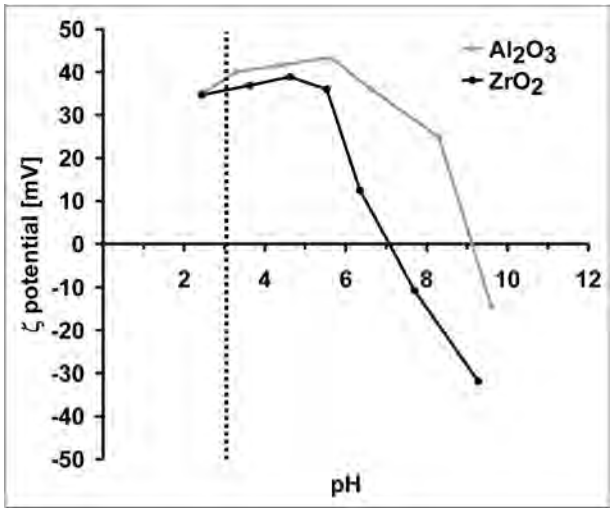

Fig. 4. Zeta potential vs. pH for alumina and zirconia nanopowders.

was 1140°C for the pure alumina powder, and it increased in the case of composite samples up to the values ranging from 1271°C to 1280°C, depending on their composition. The occurrence of the alumina phase transformation close to the above presented temperatures was confirmed by the XRD measurements (Fig. 7). In the case of pure Al_2O_3, the alpha phase was present in samples heat treated for 15 min at 1200°C, while in the composite samples, it occurred after heat treatment at 1300°C.

Besides the transformation temperature, also shrinkage rates in both temperature regions were different for the pure alumina and alumina-zironia composites. Generally, the shrinkage rates were lower in the composite samples, indicating that some hindrance was present in such systems; since the microstructures of green compacts were homogeneous (see Fig. 5) such a behaviour must be related to the presence of zirconia nanoparticles. In the effect of that, at the maximum sintering temperature of 1700°C, the alumina compact shrinkage terminated while in the composite samples it was still in progress.

The observed sintering behaviour of the composite samples resulted in their incomplete densification at the maximum sintering temperature. Fig. 8 presents the relative density of samples isothermally sintered for 15 min at temperatures ranging from 1100°C to 1300°C, and for 1 hour at 1600°C and 1700°C. An apparent density of all green samples was about 55% ± 4%, when measured from their geometrical dimensions and mass. The best densification after 1 hour of sintering at 1700°C was observed in the case of the pure alumina sample (97.84%). As it could be expected, the composite samples densified less than the pure alumina one. Amongst the composite samples, the highest density of 90.70% and the lowest one of 81.29% was achieved by the sample containing 30 vol.% and 5 vol.% of zirconia, respectively. Such a behaviour may indicate that even relatively small amount of zirconia nanoparticles interferes with the sintering of transformed alumina, and better densification of the samples containing higher amounts of zirconia could be attributed to the positive impact of zirconia nanoparticles on pore size distributions; a tendency of continuous shifting the distributions towards smaller pores with the zirconia content can be visible in Fig. 5, and additionally a content of the smallest pores increases at the expense of large pores, making the pore size distributions more uniform, and as a result also a driving force for sintering should be more uniform within the compact volume.

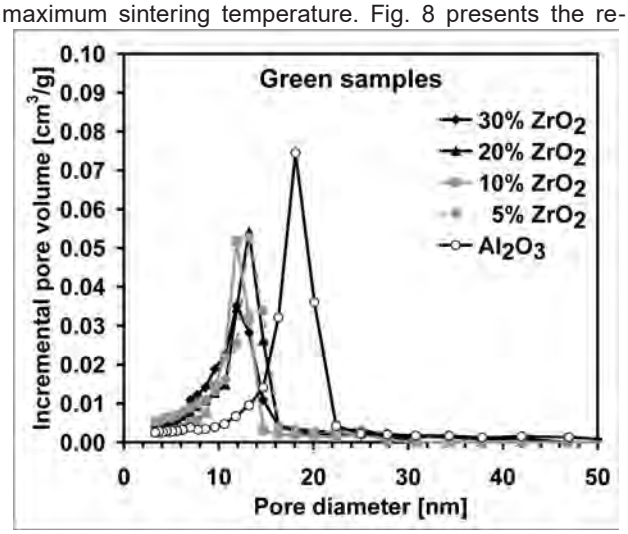

Fig. 5. Pore size distribution in green nanoalumina samples with indicated nanozirconia content.

It is interesting to note, that in the pure alumina and alumina-zirconia composite samples sintered at both 1600°C and 1700°C all remaining porosity was closed, despite its relatively high content even up to 18% in the case of sample containing 5 vol.% ZrO_2.

Changes in the microstructure, that take place during the transformation of transient aluminas to α-Al_2O_3, were monitored by pore size distribution measurements in samples heat treated at temperatures before the total pore closing (Fig. 9). The changes of pore size distribution in all alumina-zirconia composites followed the same path, showing a slight increase of pore diameters at 1100°C, when compared to the green filter pressed compact, which was accompanied by grain coarsening, as evidenced by the significant narrowing of peaks of the X-ray diffraction patterns with temperature (Fig. 7); this behaviour could be attributed to the most probable presence of differential

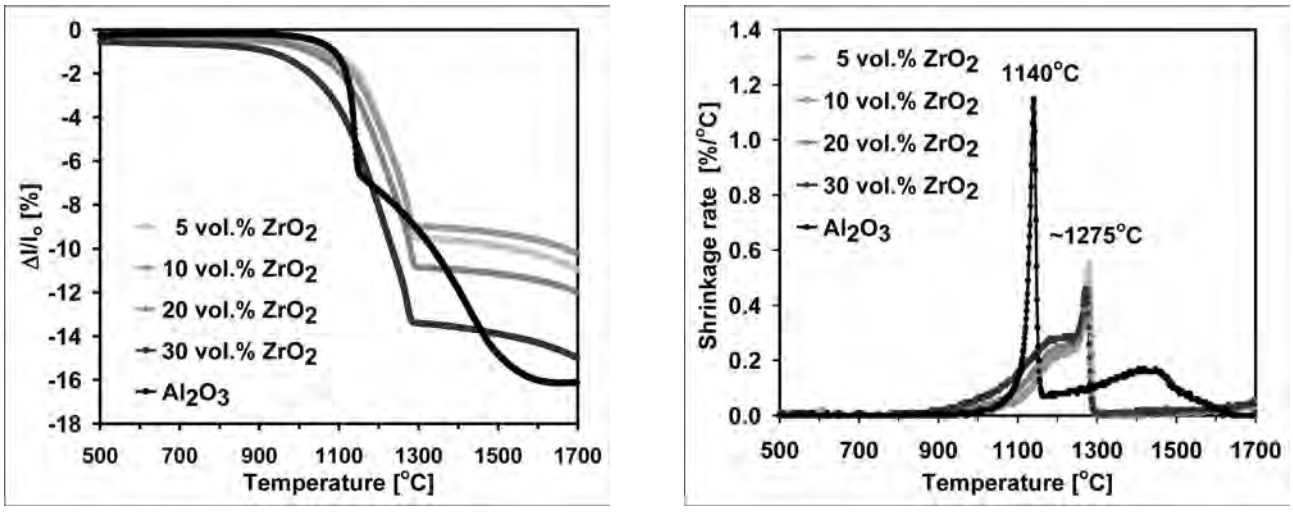

a) *b)*

Fig. 6. Shrinkage curves of filter pressed nanoalumina samples with indicated nanozirconia content: a) linear, b) derivative.

sintering effects [11–13]. The subsequent decrease of the sizes and total volume of open pores in the samples heat treated at 1200°C indicates the sintering process with no the differential component. After the phase transformation at 1275°C, the pore growth was observed in the samples sintered at 1300 °C, the range of which depended on the amount of zirconia incorporated to the composite. The lower the zirconia amount, the smaller pore growth was measured. In the case of pure alumina samples, a significant pore growth occurred at 1200°C, i.e., close to its transformation temperature of 1140 °C, and it was bigger than in any composite sample. The subsequent decrease of pore sizes and pore volume at 1300°C was related to the sintering of α-alumina phase. It is worth to note that the pore size distribution in the pure alumina samples after the transformation is narrower when compared to the composites, which may enhance their sintering.

The microstructure of sintered alumina materials is presented in Figs 10 and 11. It was impossible to distinguish between zirconia and alumina particles using the BSE mode of SEM in the partially sintered samples (1100–1300°C) due to too small crystallite size; this may also prove very homogeneous distribution of nanozirconia particles among alumina ones within green filter pressed compacts and limited nanozirconia particle agglomeration.

The transformation of transient aluminas led to visible changes in the microstructure of the samples (Figs 10b, 10c, and 11b); larger pores and vermicular grains are observed, which correspond well with the relevant pore size distributions (Fig. 9).

Grain sizes of the finally densified samples of pure alumina sintered for 2 h at 1500°C were in the range of 2–3 μm (Fig. 10d). Higher sintering temperatures led to the extensive grain growth (data not shown here).

Alumina grain sizes in the composites, that come from the final sintering temperature, were much lower (Figs 11c and 11d) which was a result of the presence of zirconia particles. The microstructure still contained a significant number of closed pores which were pinned by the zirconia grains. The considerable coarsening of zirconia grains took place due to coalescence of the particles moving along grain boundaries (Fig. 11c). In the case of composite sam-

Table 2. Volume fraction of monoclinic phase in alumina-zirconia composites sintered for 1 h at 1700°C.

	5% ZrO_2	10% ZrO_2	20% ZrO_2	30% ZrO_2
m-ZrO_2 [vol.%]	94.2	97.4	74.9	89.7

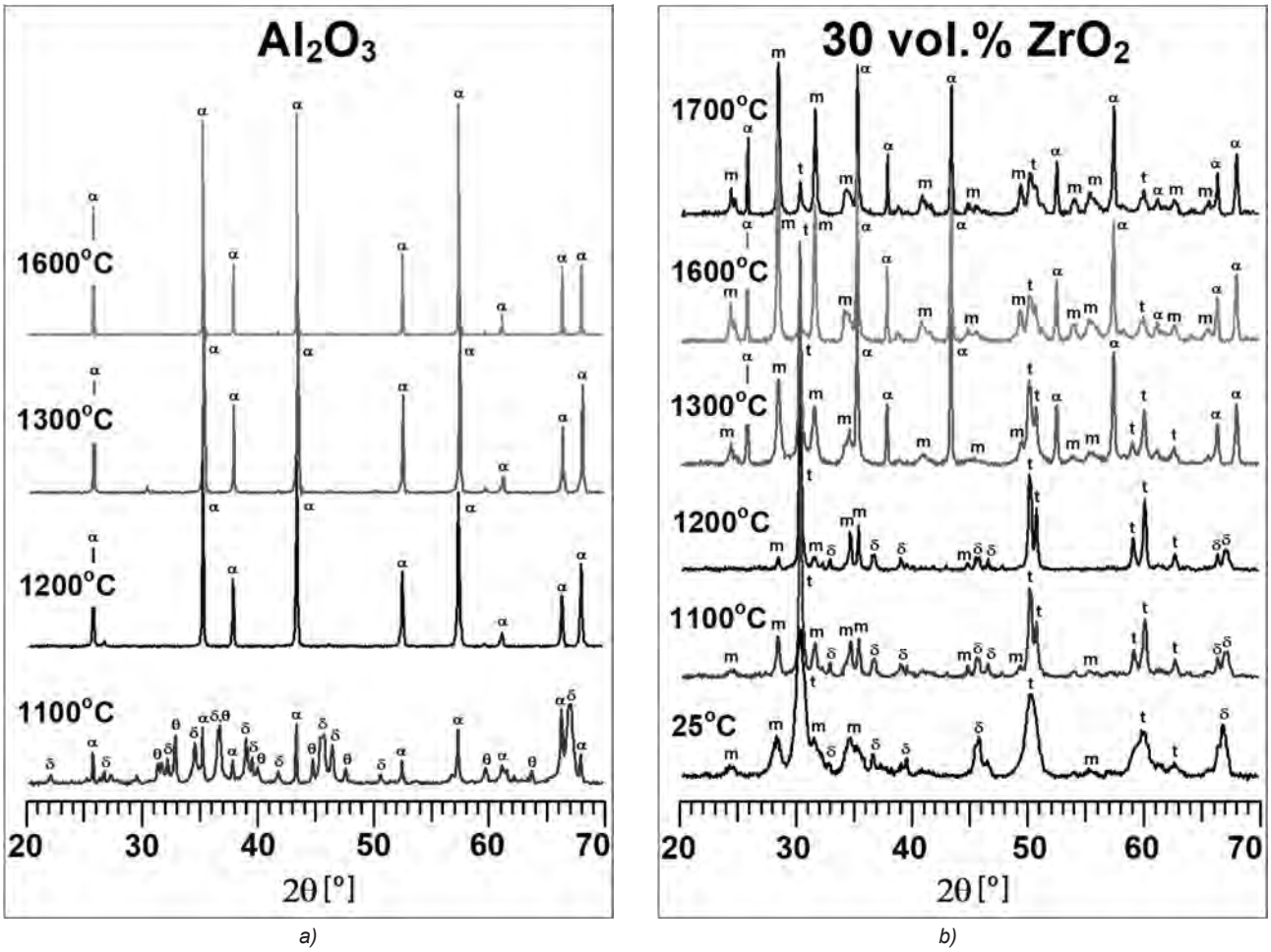

a) *b)*

Fig. 7. X-Ray diffraction patterns showing phase composition as a function of heat treatment temperature: a) pure alumina, b) alumina composite containing 30 vol.% ZrO_2; α - α-Al_2O_3, δ - δ-Al_2O_3, θ - θ-Al_2O_3, m - monoclinic ZrO_2 polymorph, t - tetragonal ZrO_2 polymorph.

ples containing higher amounts of zirconia, the sintering of them took place (Fig. 11d) which could be responsible for better densification of the composites (Fig. 8). The growth of zirconia grains was accompanied by phase transformation from the tetragonal to monoclinic polymorph. Table 2 presents volume fractions of monoclinic phase in composite samples sintered for 1 h at 1700 °C.

Mechanical properties of the samples are presented in Table 3. As it could be expected, hardness of the alumina sample was higher than the composite ones, and almost independent of their composition, which indicates that it was influenced by their relatively high porosity. Fracture toughness of the composite samples, expressed in terms of the K_{IC} coefficient, was higher than one of pure alumina, and increased with increasing the content of zirconia. However, since the majority of tetragonal zirconia grains already underwent the transformation to the monoclinic polymorph, they could not contribute to the transformation toughening mechanism (Table 2). Thus the increased toughness of the composite materials was probably a result of other mechanisms operated; crack deflection cannot be excluded.

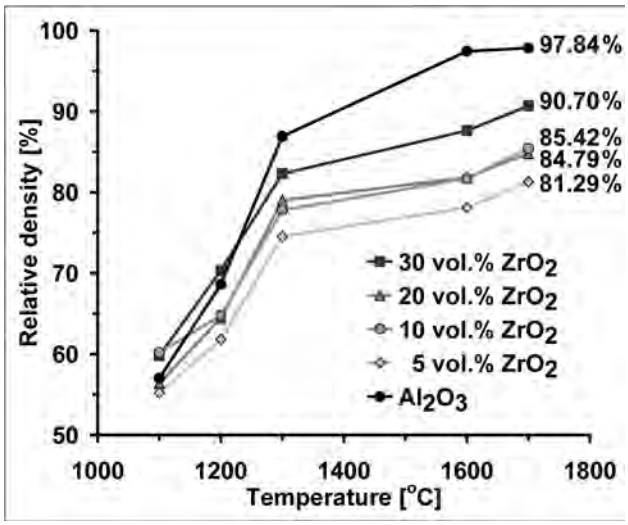

Fig. 8. Relative density of alumina materials vs. sintering temperature and composition.

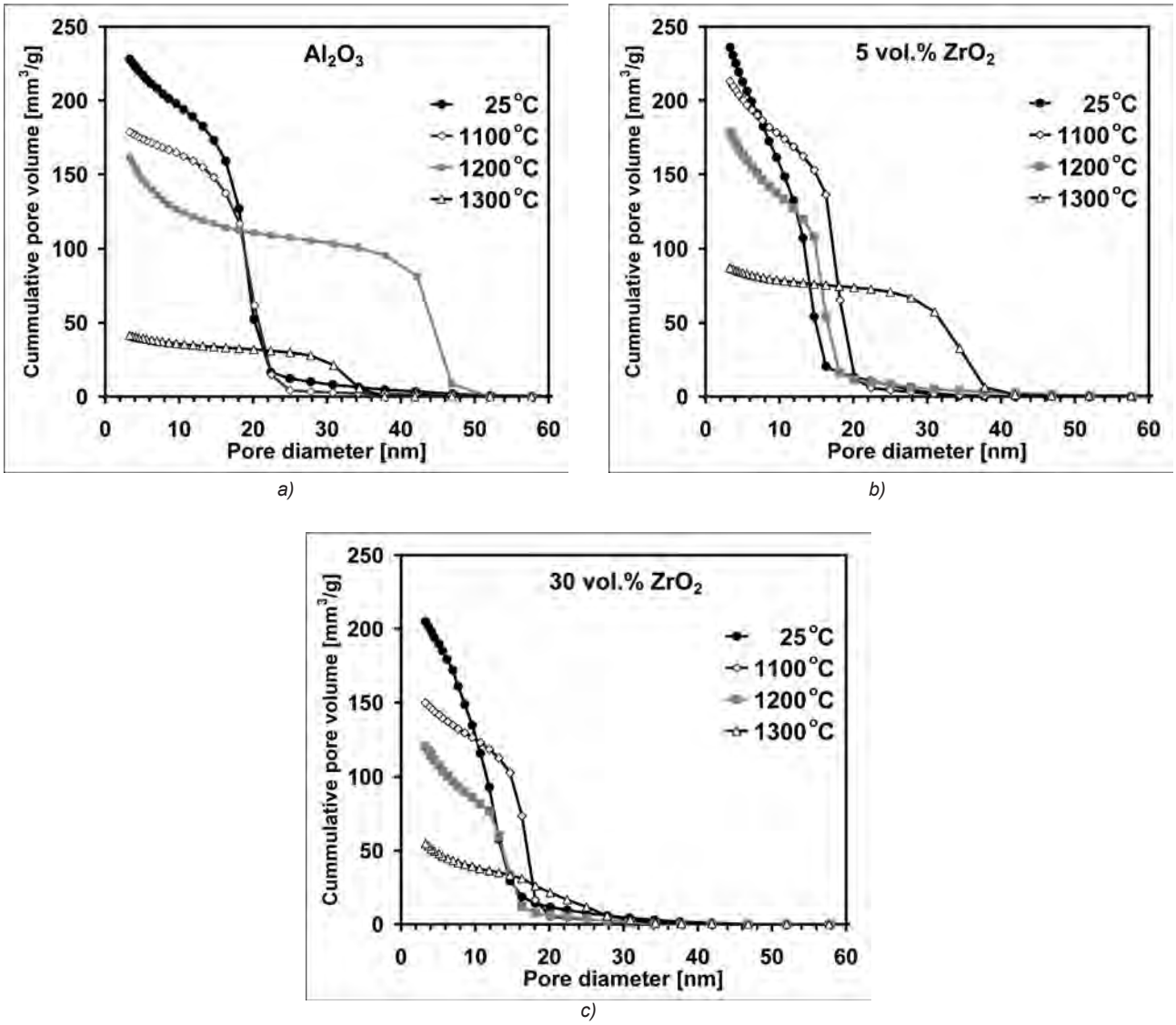

Fig. 9. Pore size distributions of alumina materials sintered at temperatures before total pore closing: a) pure alumina, b) alumina plus 5 vol.% ZrO_2 and c) alumina plus 30 vol.%; green compacts (depicted as 25°C) are also included.

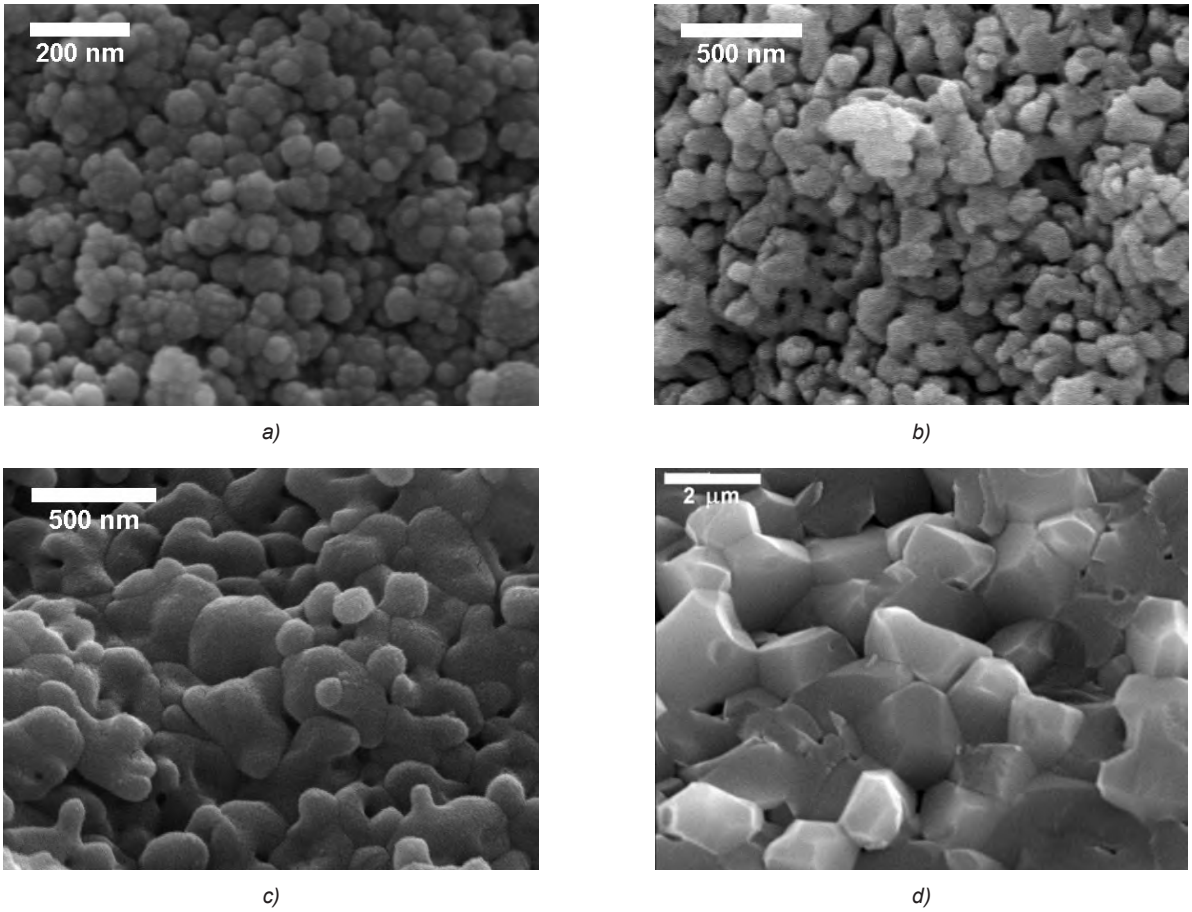

Fig. 10. SEM microphotographs, showing temperature dependence of final alumina microstructure: a) 1100°C for 15 min, b) 1200°C for 15 min, c) 1300°C for 15 min, d) 1500°C for 2 h

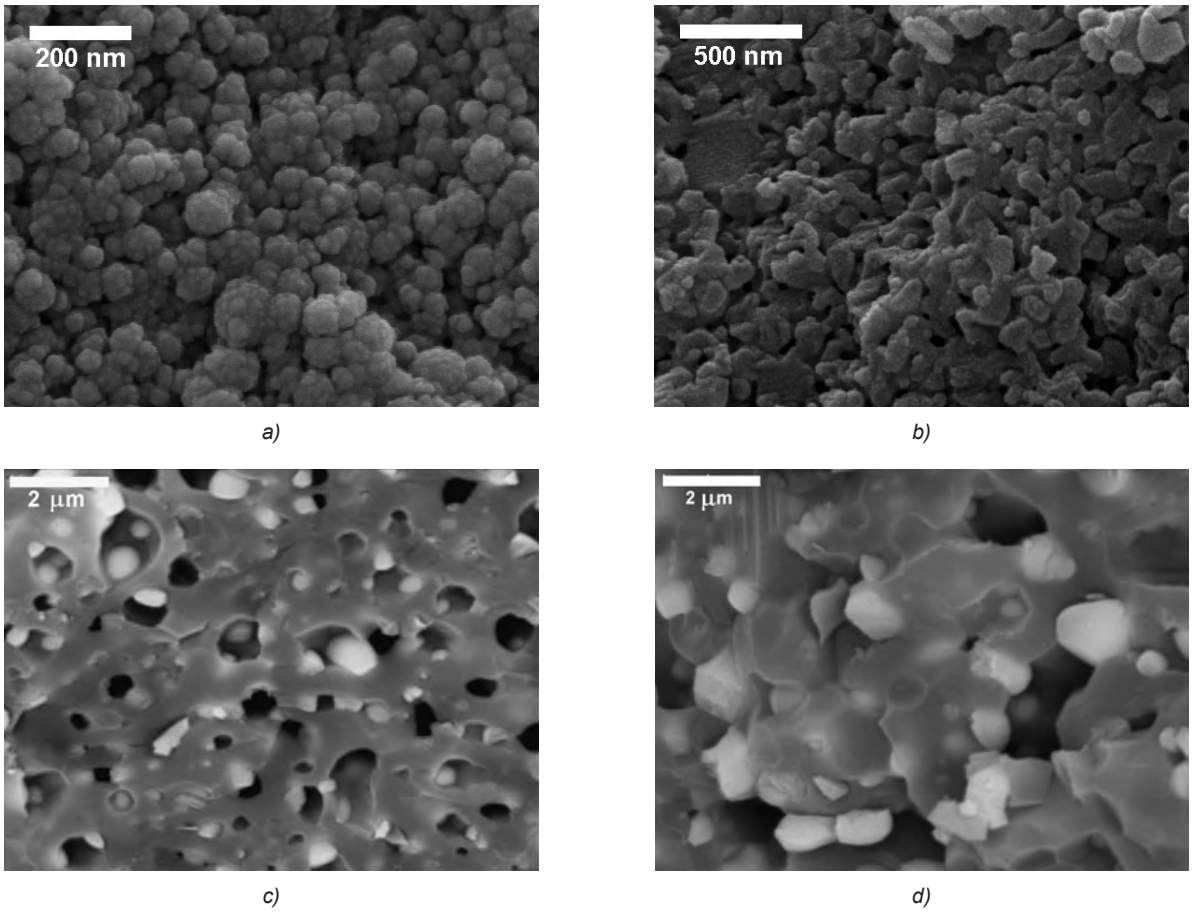

Fig. 11. SEM microphotographs, showing temperature dependence of final composite microstructure: a) 5 vol.% ZrO_2-Al_2O_3, 1100°C for 15 min, b) 5 vol.% ZrO_2-Al_2O_3, 1300°C for 15 min, c) 5 vol.% ZrO_2-Al_2O_3, 1700°C for 1 h (BSE mode), d) 30 vol.% ZrO_2-Al_2O_3, 1700°C for 1 h (BSE mode).

Table 3. Mechanical properties of sintered alumina and alumina-zirconia composites.

	Al_2O_3	5% ZrO_2-Al_2O_3	10% ZrO_2- Al_2O_3	20% ZrO_2- Al_2O_3	30% ZrO_2- Al_2O_3
Sintering temperature [°C]/ time [h]	1500/2	1700/1	1700/1	1700/1	1700/1
HV [GPa]	16.95 ±0.81	10.36 ±0.24	11.12 ±0.28	10.64 ±0.26	10.62 ±0.28
K_{IC} [MPa·m$^{0.5}$]	4.03 ±0.29	5.01 ±0.18	5.05 ±0.22	5.81 ±0.22	6.93 ±0.31
E [GPa]	396.2	269.0	326.9	296.6	241.8

4. Summary

Filter pressing of suspensions of transition alumina - zirconia nanopowders at pH 3 led to green compacts with narrow pore size distributions, which indicated their uniform microstructures. The presence of the zirconia nanoparticles shifted pore size distributions towards smaller pore within the compacts probably due to filling the pores formed among bigger alumina particles with smaller ones of the nanozirconia.

Shrinkage of all compacts started at similar temperatures c.a. 900°C, which was followed by the two-step sintering behaviour related to the transformation of transition aluminas to α-Al_2O_3, resulting in a change of the sintering rate. The transformation in transition alumina - zirconia composites was retarded of about 135°C, when compared to the alumina compacts with no zirconia additive. The transition was accompanied by growth of pores, which was the highest in the case of pure alumina, and decreased with increasing amount of zirconia.

The presence of zirconia nanoparticles strongly retarded sintering of the composites by hindering the grain boundary mobility. Closed pores in the sintered samples were pinned by zirconia grains. Better densification in the case of composites containing higher amounts of zirconia particles could be attributed to more uniform particle packing expressed by pore size distributions being narrower and containing smaller pores.

The highest toughness observed in the case of composite containing 30 vol.% was probably a result of crack deflection or crack bridging, since c.a. 90% of zirconia present in this sample was in the monoclinic form.

Acknowledgements

The authors thank the European Commission for partial supporting this work in the framework of Integrated Project "NANOKER-Structural Ceramic Nanocomposites for top-end Functional Applications", contract no: NMP3-CT-2005–515784. The research was also supported by AGH-UST, WIMiC, KCiMO under the statutory work no 11.11.160.617 in 2017.

References

[1] Hannink, R. H. J., Kelly, P. M., Muddle, B. C.: Transformation toughening in zirconia-containing ceramics, *J. Am. Ceram. Soc.*, 83, (2000), 461–487.
[2] Mayo, M. J.: Processing of nanocrystalline ceramics from ultrafine particles, *Int. Mater. Rev.*, 41, (1996), 85–115.
[3] Niihara, K.: New design concept of structural ceramics - ceramic nanocomposites, *J. Ceram. Soc. Japan*, 99, (1991), 974–982.
[4] Lange, F. F., Powder Processing Science and Technology for Increased Reliability, *J. Am. Ceram. Soc.*, 72, (1989), 3–15.
[5] Rhodes, W. H.: Agglomerate and Particle Size Effects on Sintering Yttria-Stabilized Zirconia, *J. Am. Ceram. Soc.*, 64, (1981), 19–22.
[6] Vasylkiv, O., Sakka, Y.: Synthesis and Colloidal Pressing of Zirconia Nanopowder, *J. Am. Ceram. Soc.*, 84, (2001), 2489–2494.
[7] Zych, L., Haberko, K.: Zirconia nanopowder - its shaping and sintering,. *Solid State Phenom.*, 94, (2003), 157–164.
[8] Azar, M., Palmero, P., Lombardi, M., Garnier, V., Montanaro, L., Fantozzi, G., Chevalier, J.: Effect of initial particle packing on the sintering of nanostructured transition alumina, *J. Eur. Ceram. Soc.*, 28, (2008), 1121–1128.
[9] Bowen, P., Carry, C.: From powders to sintered pieces: forming, transformations and sintering of nanostructured ceramic oxides, *Powd. Technol.*, 128 (2002), 248–255.
[10] Vasylkiv, O., Sakka, Y., Skorohod, V.V.: Low-temperature processing and mechanical properties of zirconia and zirconia-alumina nanoceramics, *J. Am. Ceram. Soc.*, 86, (2003), 299–304.
[11] de Jonge, L. C., Rahaman, M. N.: Chapter 4.1 Sintering of Ceramics, in *Handbook of Advanced Ceramics*, Somiya, S. et al. (Eds.), Academic Press, 2003.
[12] Pyda, W., Gani, M. S. J.: Microstructure and mechanical properties of spherical zirconia-yttria granules, *J. Mater. Sci.*, 30, (1995), 2121–2129.
[13] Pyda, W.: The relation between preparation, microstructure and mechanical properties of spherical yttria-zirconia powders, *J. Eur. Ceram. Soc.*, 17, (1997), 121–127.

♦

Received 15 August 2017, accepted 1 September 2017.